Liquid Crystals
Publication details, including instructions for authors and subscription information:
http://www.informaworld.com/smpp/title~content=t713926090

Synthesis and X-ray investigation of liquid crystalline polymers containing laterally methyl-substituted tolane-based mesogenic side groups

Chang-Jyh Hsieh[a]; Ging-Ho Hsiue[a]
[a] Department of Chemical Engineering, National Tsing Hua University Hsinchu, Taiwan, Republic of China

To cite this Article Hsieh, Chang-Jyh and Hsiue, Ging-Ho(1995) 'Synthesis and X-ray investigation of liquid crystalline polymers containing laterally methyl-substituted tolane-based mesogenic side groups', Liquid Crystals, 18: 2, 263 — 269
To link to this Article: DOI: 10.1080/02678299508036622
URL: http://dx.doi.org/10.1080/02678299508036622

LIQUID CRYSTALS, 1995, VOL. 18, NO. 2, 263–269

Synthesis and X-ray investigation of liquid crystalline polymers containing laterally methyl-substituted tolane-based mesogenic side groups

by CHANG-JYH HSIEH and GING-HO HSIUE*
Department of Chemical Engineering, National Tsing Hua University,
Hsinchu, Taiwan 30043, Republic of China

(*Received 1 April 1994; accepted 1 May 1994*)

A series of polymethacrylates containing laterally methyl-substituted 4-alkoxy-4′-nitrotolane, 4-alkoxy-4′-cyanotolane, and 4-alkoxy-4′-trifluoromethyltolane as mesogenic side groups are presented. The thermal behaviours of the prepared compounds were characterized by differential scanning calorimetry, optical polarized microscopy and X-ray diffraction. All of the obtained methacrylate monomers exhibit no mesophase, while most of the synthesized polymers reveal enantiotropic mesomorphism. The polymer containing 4-propyloxy-2′-methyl-4′-nitrotolane side groups was the only one to show no mesomorphic behaviour. The spacer length and the nature of terminal group have a profound influence on the type of mesophase formed and the thermal stability. Incorporation of a lateral methyl-substituent into the mesogenic groups reduces the thermal stabilities of the mesophases. X-ray diffraction reveals that polymers with a smectic A or smectic E phase have the inclination to form a bilayer structure. Increasing the temperature within the smectic phase range, the intermolecular spacing increases while the layer spacing decreases. On the other hand, introducing a lateral substituent into the mesogenic side groups leads to increase in both layer and intermolecular spacing.

1. Introduction

Since the introduction of the spacer concept, a large variety of side-chain liquid crystalline polymers (side-chain LCPs) have been synthesized and characterized [1]. These polymers combine the properties of liquid crystals as anisotropic fluids with the mechanical properties of polymers, in particular they present a glass transition (T_g) below which the molecular organization may be frozen. The application of side-chain LCPs in the field on non-linear optics was first reported at the beginning of the 1980s [1–8]. Meredith *et al.* demonstrated that doping 4-dimethylamino-4′-nitrostilbene (DANS) in a LCP matrix could obtain higher second order susceptibility than in an amorphous polymer matrix [2]. DeMartino *et al.*, reported possessing covalently attached non-linear chromophores would improve solubility and stability of materials [4]. In order to give high non-linearity, the molecular design of the chromophore is usually inclined toward as a donor–acceptor system. However, the strong intermolecular dipole moment giving rise to the antiparallel correlation, resulted in a centrosymmetric structure [7, 8]. According to the literature, introducing a non-symmetrical substituted group into organic crystals will destroy the symmetry of organic crystals and consequently give large non-linearity [7].

The aim of this study is to investigate the influence of a lateral methyl-substituent on the thermal behaviour of the side-chain liquid crystalline polymethacrylates containing tolane-based mesogens. All polymers were characterized by differential scanning calorimetry (DSC) and optical polarized microscopy. Furthermore, X-ray diffraction was used for an accurate identification of the mesophase and elucidation of the structure correlation.

2. Synthesis

The synthetic routes used for the preparation of side-chain liquid crystalline polymethacrylates are outlined in the scheme. The starting material 4-bromo-3-methylphenol could be prepared either by the decomposition of diazonium sulphate of 4-bromo-3-methylaniline or by direct bromination of *m*-cresol in chloroform solution. In general, the former method could be achieved with high yields and without side reactions [9, 10]. After the etherification reactions, the 3-substituted-4-bromo-1-(ω-hydroxyalkoxy) benzenes were coupled with 2-methyl-3-butyn-2-ol in the presence of a palladium complex and a copper (I) salt [11]. The resulting alkynols were then deprotected and coupled with

---

* Author for correspondence.

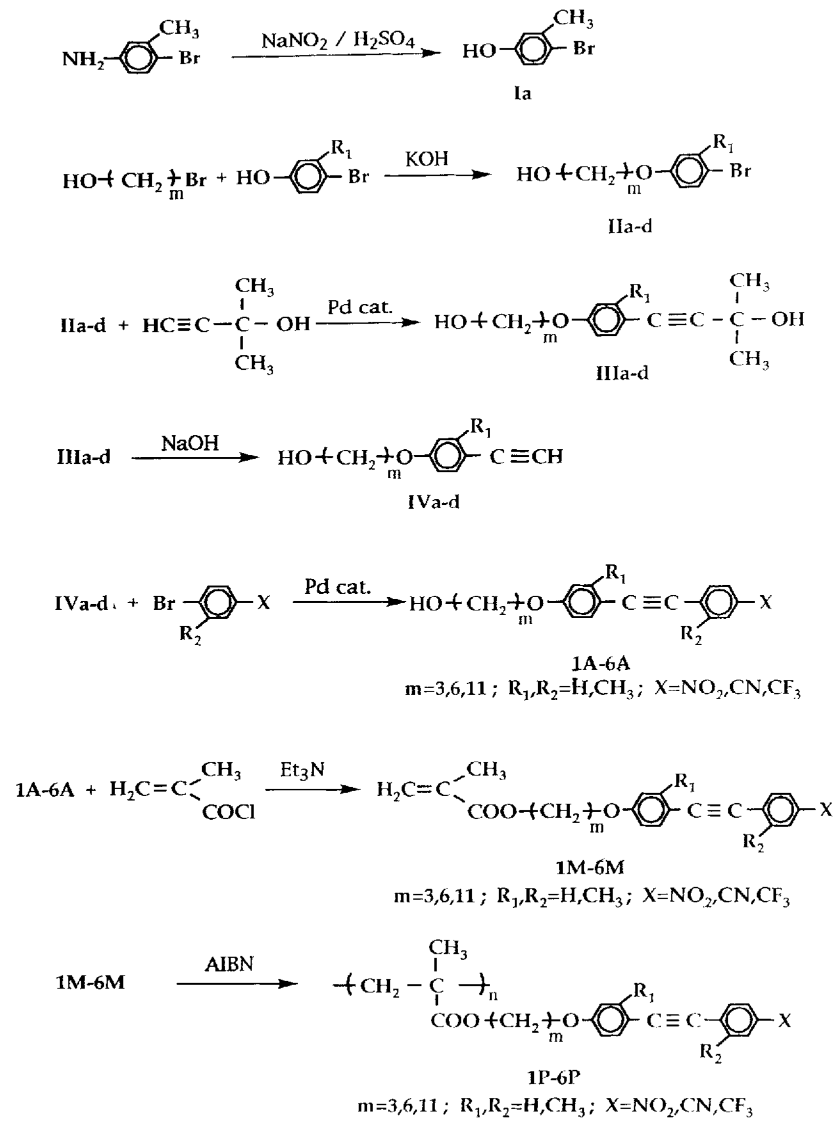

Scheme. Synthesis of side chain liquid crystalline polymers **1P–6P**.

corresponding aryl halides. The methacrylate monomers were synthesized by simple esterification reactions of the corresponding alcohols with methacryloyl chloride. The polymethacrylates were eventually obtained via a free radical polymerization of the prepared monomers using AIBN as an initiator.

Synthetic details of the above reactions are described in experimental section.

3. Results and discussion

3.1. *Thermal behaviour*

The thermal transitions of the unsymmetrical tolane compounds **1A–6A** are listed in table 1. The mesophases of most of the synthesized compounds are less thermally stable in comparison with the corresponding unsubstituted compounds [8]. In some cases, the mesophase was even destroyed. The phase transitions and thermodynamic parameters of the methacrylate monomers **1M–6M** are also summarized in table 1. All of the monomers showed no liquid crystalline behaviour, despite that most of their corresponding hydroxy-terminated precursors exhibited mesomorphism. It seems that the bulky methacrylate group depresses the formation of a liquid crystalline phase.

The polymethacrylates were synthesized via free radical polymerizations of the corresponding monomers using AIBN as an initiator. All polymers were purified by several recrystallizations and checked for any traces of unreacted monomers by GPC measurements. The molecular weights and the thermal transitions of the obtained polymers are reported in table 2. The molecular weights of all polymers are higher than 10 000. It is well-documented that above a certain molecular weight the phase transitions of LCPs are no longer molecular-weight dependent [12, 13]. From this table, it is found that all of

Table 1. Phase transitions (°C) and corresponding enthalpy changes in brackets ($J\,g^{-1}$) of compounds **1A–6A** and methacrylate monomers **1M–6M**.

Compound	m†	R_1	R_2	X	Phase transitions‡
1A	3	H	CH_3	NO_2	C 72·9 RC 123·5 (111·3) I I 74·7 (0·6) N 66·9 (46·6) C
2A	6	H	CH_3	NO_2	C 128·4 (161·6) I I 111·6 (157·2) C
3A	11	H	CH_3	NO_2	C 80·7 (117·0) I I 73·3 (6·0) N 43·5 (88·6) C
4A	11	CH_3	H	NO_2	C 1·0 RC 70·0 (73·0) I I 42·0 (2·9) N–9·0 (7·4) C
5A	11	CH_3	H	CN	C 92·9 (140·7) I I 65·9 (134·6) C
6A	11	CH_3	H	CF_3	C 80·7 (89·6) I I 66·2 (83·8) C
1M	3	H	CH_3	NO_2	C 90·9 (79·8) I I 73·2 (71·5) C
2M	6	H	CH_3	NO_2	C 5·8 RC 62·4 (80·5) I I 0·3 (15·2) C
3M	11	H	CH_3	NO_2	C 86·9 (138·1) I I 69·8 (136·3) C
4M	11	CH_3	H	NO_2	C 75·0 (87·0) I I 53·3 (81·1) C
5M	11	CH_3	H	CN	C 80·6 (95·7) I I 55·6 (94·7) C
6M	11	CH_3	H	CF_3	C 70·8 (100·4) I I 38·2 (91·7) C

† m, R_1, R_2, X, according to the scheme.

‡ C, crystalline; RC, recrystalline; S_E, smectic E; N, nematic; I, isotropic; first line of data obtained from second heating scans; second line of data obtained from cooling scans.

the polymers exhibit mesomorphic behaviour except **1P** and **7P** (due to their shorter flexible side chain). In spite of such a rigid rod-like mesogen in the side-chain LCPs, there was no side-chain crystallization occurring in all cases even though the spacer contained 11 methylene units. This is an important feature for practical applications [1].

Polymers **1P–3P** containing the same 2′-methyl-4′-nitrotolane as side groups have different lengths of alkoxy spacer. They also reveal distinct thermal behaviour. Polymer **1P** shows a T_g on heating and cooling, and polymer **2P** presents a T_g and an enantiotropic nematic phase, while polymer **3P** exhibits a T_g and an enantiotropic smectic phase. These results demonstrate that a longer alkoxy spacer cannot only increase the isotropization temperature but also lead to the formation of a more ordered mesophase. The spacer effect is also present in another series of polymers **7P–9P** which contain 4′-nitrotolane in their side chains.

Polymers **4P–6P** contain the same spacer length and tolane core structure but differ in their terminal groups. Polymers **4P** and **6P** exhibit a nematic phase while polymer **5P** shows a smectic A phase. It is obvious that the nature of the terminal group plays a decisive role on the type of mesophase. In comparison with polymers **9P–11P**, it seems that introducing a 2-methyl lateral substituent into the mesogenic cores of the polymers not only dramatically decreases their isotropization temperatures, but also changes the type of mesophase in case of polymers **4P** and **6P**. To study the effect of the position of the lateral methyl substituent, polymers **3P** and **4P** were the materials of choice. Both polymers have the same spacer length and tolane-core structure, while differing in the position of the lateral methyl-substituent, and possess similar T_g values. However, polymer **3P** shows a much wider mesomorphic temperature range and a more ordered mesophase. The result demonstrates that the lateral methyl-substituent which is placed near the polymer backbone shows much greater steric effect than the other position.

3.2. *X-ray investigation*

X-ray studies were performed to realize further how the terminal groups and lateral substituents affect the microscopic molecular structure of mesophase. Figure 1 depicts the X-ray diffraction scans of polymers **9P–11P** and their corresponding laterally substituted polymers **3P–6P**. The corresponding diffraction data are listed in table 3. Curve *A* is the X-ray diffraction diagram of polymer **9P**. A broad reflection was observed at about 4·46 Å which corresponds to the lateral spacing of two mesogenic side groups. In addition, a sharp first order reflection was found at 40·5 Å along with a second order reflection at 20·3 Å which correspond to the smectic layer spacings. The mesophase of polymer **9P** is classified as a smectic A phase, which agrees with the textual observation by polarizing optical microscopy. It is interesting to note that the average layer spacing is approximately 1·3 times greater than the fully extended molecular length. This is regarded as an interdigitated bilayer smectic structure resulting from the strong dipole moment of molecules. The bilayer structures are usually present in materials that contain a terminal nitro- or cyano-group [14, 15]. This is also confirmed by X-ray diffraction of polymer **10P** (see figure 1, curve *B*). Curve *C* is the X-ray diffraction scan of polymer **11P**; several reflections were found as below. The small angle reflections appearing at 40·1 Å (first order), 19·4 Å (second order) and 12·6 Å (third order) represent the smectic layer spacings. In the wide angle range, there are three sharp reflections which correspond to the orthorhombic array within the lattice of a smectic E mesophase. To our knowledge, this is the first example of a highly ordered smectic E phase exhibiting the interdigitated bilayer structure. Curves *D–G* are the X-ray diffraction scans of polymers **3P–6P**. It is apparent that the intermolecular spacings of these polymers increase as the lateral

Table 2. Molecular weight, phase transitions (°C) and corresponding enthalpy changes in brackets ($J\,g^{-1}$) of polymers **1P–11P**.

Polymer	*m*†	R_1	R_2	*X*	GPC $10^{-3}\bar{M}_n$	GPC $\bar{M}_w/\bar{M}_n$	Phase transitions‡
1P	3	H	CH_3	NO_2	15·7	1·4	g 82·9 I I 79·4 g
2P	6	H	CH_3	NO_2	23·7	2·7	g 45·3 N 76·5 (1·6) I I 66·0 (1·4) N 41·8 g
3P	11	H	CH_3	NO_2	41·9	1·6	g 24·0 S_A 97·0 (5·7) I I 87·0 (5·3) S_A 23·0 g
4P	11	CH_3	H	NO_2	24·4	1·9	g 23·3 N 43·5 (4·9) I I 31·2 (3·5) N 19·7 g
5P	11	CH_3	H	CN	28·5	2·0	g 19·7 S_A 78·6 (7·4) I I 72·1 (6·6) S_A 18·0 g
6P	11	CH_3	H	CF_3	10·5	2·5	g 19·9 N 37·4 (3·4) I I 32·7 (2·4) N 15·6 g
7P§	3	H	H	NO_2	12·9	1·9	g 75·0 I I 71·3 g
8P§	6	H	H	NO_2	36·5	1·6	g 47·7 N 78·6 (1·8) I I 70·3 (1·7) N 42·7 g
9P§	11	H	H	NO_2	18·2	2·1	g 19·7 S_A 115·5 (6·7) I I 108·7 (6·4) S_A 16·4 I
10P§	11	H	H	CN	30·2	1·8	g 20·6 S_A 133·0 (7·5) I I 125·4 (7·1) S_A 18·4 g
11P§	11	H	H	CF_3	24·5	2·1	g 25·0 S_E 122·9 (22·4) I I 113·8 (22·7) S_E 28·6 g

† *m*, R_1, R_2, *X*, according to the scheme.

‡ C, crystalline; g, glass; S_E, smectic E; S_A, smectic A; N, nematic; I, isotropic; first line of data obtained from second heating scans; second line of data obtained from cooling scans.

§ Data obtained from [8].

substituent is introduced into the tolane based mesogens. The polymers **3P** and **5P** are the only two polymers that retain their anti-parallel smectic structure. Furthermore, in spite of the steric hindrance effect due to the lateral substituent, their smectic layer spacings are 2–3 Å longer than their corresponding unsubstituted polymers.

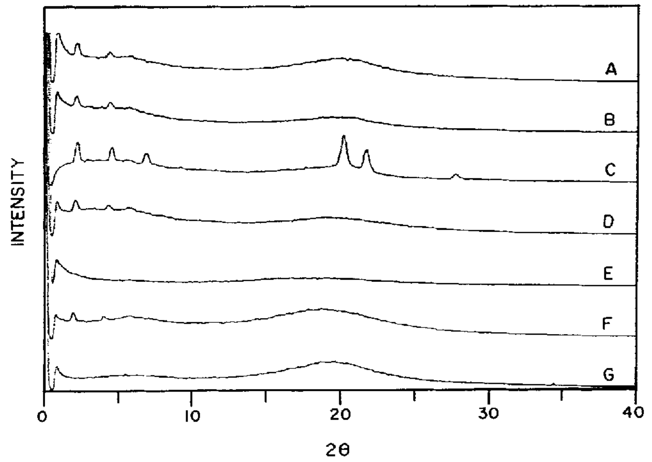

Figure 1. X-ray diffractogram of the polymers: (A) **9P**, (B) **10P**, (C) **11P**, (D) **3P**, (E) **4P**, (F) **5P**, and (E) **6P**.

The smectic layer spacing and intermolecular distance for polymer **9P** are depicted as a function of temperature and shown in figure 2. As the temperature increases, the intermolecular spacing slightly increases while the smectic layer spacing decreases. This could be due to the increase in the mobility of the polymer with the increasing temperature [16].

4. Conclusions

Spacer length, the type of terminal group, and the lateral substitution, have a profound influence on the thermal stability and type of the mesophase formed by a side-chain liquid crystalline polymer. The polymers with longer spacers tend to form a more ordered mesophase with a wider mesomorphic temperature range. Incorporation of the lateral methyl substituent into the tolane-core structure reduces both the thermal stabilities of nematic and smectic phases, in particular the smectic phase is more severely affected. In addition, the positions of the substituent also play an important role on the thermal stability of the mesophase. The polymer with a methyl substituent at the phenyl ring near the polymer backbone causes a greater depression of phase transition temperatures and thermal stability of the mesophase. Furthermore, X-ray studies

Table 3. X-ray scattering results for the side chain liquid crystalline polymethacrylates at 30°C.

Polymer	Layer spacing/Å First order	Second order	Third order	Calculated length of full extended molecules/Å	Intermolecular distance/Å
9P	40·5	20·3	—	30·9	4·46
10P	41·1	20·5	—	31·5	4·48
11P	40·1	19·4	12·6	21·2	4·39
3P	42·2	21·0	—	30·9	4·67
4P	—	—	—	30·9	4·83
5P	44·1	22·0	—	31·5	4·68
6P	—	—	—	31·2	4·60

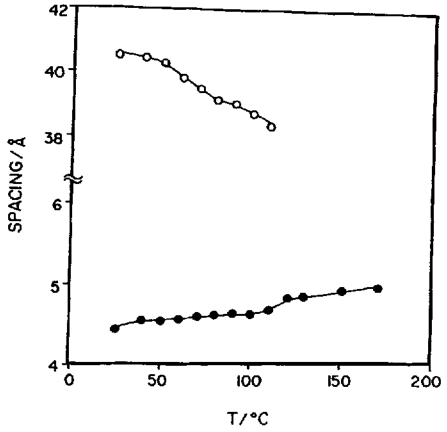

Figure 2. Variation of the layer spacing (○) and intermolecular distance (●) with temperature of the polymer **9P**.

found that the polymers containing a donor–acceptor type mesogen formed a smectic layer with an anti-parallel arrangement owing to the strong permanent dipole moment. Incorporation of a lateral substituent into the mesogenic core increases the intermolecular distance and layer spacing and hence leads to the formation of a less-ordered mesophase.

The explanation for these concluding remarks is clearly addressed in 'Results and discussion' section.

5. Experimental

5.1. *Materials*

Bis(triphenylphosphine)palladium(II) chloride, triphenylphosphine, 2-methyl-3-butyn-2-ol (all from Janssen, Belgium), copper(I) iodide (from Merck U.K. Ltd) and all other reagents (from Aldrich) were used as received. Tetrahydrofuran was first refluxed over potassium and then distilled under nitrogen. Chloroform was dried by refluxing over calcium hydride followed by distillation. 2,2′-Azoisobutyronitrile (AIBN) (from Janssen) was freshly recrystallized from methanol (below 40°C).

5.2. *Techniques*

^{1}H NMR spectra were obtained with a Bruker AM-400 spectrometer. All spectra were recorded from $CDCl_3$ solutions with TMS as the internal standard. IR spectra were measured using a Perkin–Elmer 842 infrared spectrometer. Purity was determined by high performance liquid chromatography (HPLC) with a Spectra-Physics LC instrument. The molecular weights of the polymers were determined by gel permeation chromatography (GPC) with an Applied Biosystems series 400 instrument equipped a Viscotek differential/viscometer detector. A set of four Ultrastyragel linear columns was used with tetrahydrofuran as eluent at a flow rate of 1 ml min^{-1}. The number- and weight-average molecular weight ($\bar{M}_n$ and $\bar{M}_w$) were determined relative to polystyrene standards. A Seiko 5200 differential scanning calorimeter (DSC) equipped with a 5200H computer system was used to determine the thermal transitions that were taken at the maximum of the endothermic or exothermic peaks. In all cases, heating and cooling rates were 10°C min^{-1}. Glass transition temperatures (T_g) were read at the middle of the change in heat capacity. A Nikon Microphot-FX optical polarizing microscope equipped with a Mettler FP 82 hot stage and a Mettler FP 80 central processor was used to observe thermal transitions and anisotropic textures. X-ray diffraction patterns were obtained with a Rigaku R-AXIS ICC diffractometer using nickel-filtered CuK_α radiation equipped with an image plate system. Samples were inserted into a 2·0 mm diameter circular ring clamped between two sheets of amorphous Kaptan films and attached to a metal heating block. The temperature stability in these experiments was ± 0·1°C.

5.3. *Synthesis of monomers*

The synthetic procedures for methacrylate monomers are outlined in the scheme. All of the monomers were synthesized by similar methods. A typical procedure is shown below the monomer **4M**.

5.3.1. *4-Bromo-3-methylphenol*

This compound was prepared by the decomposition of diazonium sulphate of 4-bromo-3-methylaniline by the method previously reported [9]. Yield: 75 per cent of colourless oil. ^{1}H NMR ($\mathrm{CDCl_3}$, TMS) δ 2·32 (s, 3 H, $-\mathrm{CH_3}$), 6·55, 6·74 and 7·32 (d, s and d, 3 H, aromatic protons).

5.3.2. *4-Bromo-1-(11-hydroxyundecanyloxy)-3-methylbenzene*

A mixture of 4-bromo-3-methylphenol (10·8 g, 57·8 mmol), potassium hydroxide (3·2 g, 57·8 mmol) and dimethyl sulphoxide (100 ml) was heated to 65°C. Then 11-bromo-1-undecanol (16·0 g, 63·6 mmol) was added dropwise [8, 17]. The solution was stirred at 65°C for 18 h, then cooled to room temperature. The solvent was removed under reduced pressure. The crude product was dissolved in ethyl acetate and the extract washed with dilute potassium hydroxide, water, and dried over anhydrous magnesium sulphate. After solvent was removed in a rotary evaporator, the residue was purified by column chromatography using silica gel with 10:1 chloroform/tetrahydrofuran as eluent to yield 17·7 g (85·6 per cent) of colourless oily product. ^{1}H NMR ($\mathrm{CDCl_3}$, TMS) δ 1·34–1·77 (m, 18 H, $-(\mathrm{CH_2})_9-$), 2·38 (s, 3 H, Ph–$\mathrm{CH_3}$), 3·63 (t, 2 H, $-\mathrm{O{-}CH_2}-$), 3·88 (t, 2 H, $-\mathrm{CH_2{-}OPh}$), 6·58–7·38 (m, 3 H, aromatic protons).

5.3.3. *4-(3-Hydroxy-3-methyl-1-butynyl)-1-(11-hydroxyundecanyloxy)-3-methylbenzene*

To a solution of 4-bromo-1-(11-hydroxyundecanyloxy)-3-methylbenzene, (23·6 g, 66·0 mmol), 2-methyl-3-butyn-2-ol (6·7 g, 79·0 mmol) and dry triethylamine (50 ml) in tetrahydrofuran (100 ml), bis(triphenylphosphine)palladium(II) chloride (0·33 g), copper(I) iodide (0·33 g) and triphenylphosphine (0·66 g) were added [11]. The mixture was heated to 60°C overnight. After filtration to remove precipitated material, the solvent was evaporated under reduced pressure. The crude product was purified by column chromatography using silica gel with 6:1 chloroform/tetrahydrofuran as eluent to yield 16·7 g (70·2 per cent) of white crystals. m.p. 35·5°C. ^{1}H NMR ($\mathrm{CDCl_3}$, TMS) δ 1·29–1·82 (m, 18 H, $-(\mathrm{CH_2})_9-$), 1·63 (s, 6 H, $-(\mathrm{CH_3})_2$), 2·38 (s, 3 H, Ph–$\mathrm{CH_3}$) 3·64 (t, 2 H, $-\mathrm{O{-}CH_2}-$), 3·93 (t, 2 H, $-\mathrm{CH_2{-}OPh}$), 6·63–7·30 (m, 3 H, aromatic protons).

5.3.4. *[4-(11-Hydroxyundecanyloxy)-3-methylphenyl]-acetate*

4-(3-Hydroxy-3-methyl-1-butynyl)-1-(11-hydroxyundecanyloxy)-3-methylbenzene (15·5 g, 43·0 mmol) was dissolved in anhydrous toluene (150 ml) in a reaction vessel equipped with a Dean–Stark trap and a reflex condenser, and then the sodium hydroxide (1·7 g, 43·0 mmol) added [11]. The mixture was heated at reflux for 3 h. The mixture was then cooled to room temperature, shaken with water, and the organic layer dried over anhydrous magnesium sulphate. Toluene was removed and the resulting solid was purified by column chromatography using silica gel with 12:1 chloroform/tetrahydrofuran as eluent to yield 9·2 g (70·5 per cent) of light yellow oily product. ^{1}H NMR ($\mathrm{CDCl_3}$, TMS) δ 1·29–1·78 (m, 18 H, $-(\mathrm{CH_2})_9-$), 2·42 (t, 3 H, Ph–$\mathrm{CH_3}$), 3·18 (s, 1 H, $-\mathrm{C{\equiv}C{-}H}$), 3·64 (t, 2 H, $-\mathrm{O{-}CH_2}-$), 3·94 (t, 2 H, $-\mathrm{CH_2}$–OPh), 6·65–7·38 (m, 3 H, aromatic protons).

5.3.5. *1-[4-(11-Hydroxyundecanyloxy)-3-methylphenyl]-2-(4′-nitrophenyl)acetylene*

To a solution of [4-(11-hydroxyundecanyloxy)-3-methylphenyl]acetylene (3·0 g, 10·0 mmol) and 4-bromonitrobenzene (2·4 g, 12·0 mmol) in dry triethylamine (10 ml) and tetrahydrofuran (40 ml), bis(triphenylphosphine)palladium(II) chloride (0·05 g), copper(I) iodide (0·05 g) and triphenylphosphine (0·10 g) were added. The mixture was heated at reflux overnight, then cooled to room temperature. After filtration to remove precipitated material, the solvent was evaporated under reduced pressure. The crude product was purified by column chromatography using silica gel with 30:1 chloroform/tetrahydrofuran as eluent to yield 3·0 g (71·8 per cent) of yellow crystals. ^{1}H NMR ($\mathrm{CDCl_3}$, TMS) δ 1·25–1·80 (m, 18 H, $-(\mathrm{CH_2})_9-$), 2·48 (s, 3 H, Ph–$\mathrm{CH_3}$), 3·64 (t, 2 H, $-\mathrm{O{-}CH_2}-$), 3·94 (t, 2 H, $-\mathrm{CH_2{-}OPh}$), 6·64–8·14 (m, 7 H, aromatic protons). The yields for all synthesized compounds **1A–6A** together with their phase transition temperatures are presented in table 1.

5.3.6. *1-[4-(11-Methacryloyloxyundecanyloxy)-3-methylphenyl]-2-(4′-nitrophenyl)acetylene*

1-[4-(11-Hydroxyundecanyloxy)-3-methylphenyl]-2-(4′-nitrophenyl)acetylene (1·99 g, 4·70 mmol) was dissolved in a mixture of dried tetrahydrofuran (30 ml) and triethylamine (1·01 g, 9·98 mmol). After the solution was cooled in an ice–water bath to 0°C, and methacryloyl chloride (0·74 g, 7·05 mmol) was added dropwise. The mixture was allowed to warm slowly to room temperature and stirred overnight. The product was obtained by being poured into water, filtered, dried under vacuum, and purified by column chromatography using silica gel with chloroform as eluent to yield 1·97 g (85·4 per cent) of yellow crystals. The yields, ^{1}H NMR chemical shifts, and phase transition temperatures of monomers **1M–6M** are summarized in tables 1 and 4.

5.4. *Synthesis of polymethacrylates*

The free radical polymerizations of the monomers were carried out in a Schlenk tube under nitrogen. The polymerization tube, which contained a chloroform

Table 4. Characterization of methacrylate monomers **1M–6M**.

Monomer	Yield per cent	400 MHz ^{1}H NMR ($\mathrm{CDCL_3}$, TMS, δ/ppm)
1M	92	1·95 (s, 3 H, $-\mathrm{C\underline{H}_3}$), 2·19 (m, 2 H, $-\mathrm{CH_2{-}CH_2{-}C\underline{H}_2}-$), 2·59 (s, 3 H Ph–$\mathrm{C\underline{H}_3}$), 4·10 (t, 2 H, $-\mathrm{C\underline{H}_2}$–OPh), 4·36 (t, 2 H, –COO–$\mathrm{C\underline{H}_2}$–), 5·57 and 6·11 (2s, 2 H, $\mathrm{CH_2}$=), 6·89–8·11 (m, 7 H, aromatic protons).
2M	89	1·45–1·84 (m, 8 H, $-(\mathrm{C\underline{H}_2})_4-$), 1·95 (s, 3 H, $-\mathrm{C\underline{H}_3}$), 2·59 (s, 3 H, Ph·$\mathrm{C\underline{H}_3}$), 3·99 (t, 2 H, $-\mathrm{C\underline{H}_2}$–OPh), 4·16 (t, 2 H, –COO–$\mathrm{C\underline{H}_2}$–), 5·55 and 6·10 (2s, 2 H, $\mathrm{C\underline{H}_2}$=), 6·88–8·10 (m, 7 H, aromatic protons).
3M	92	1·30–1·79 (m, 18 H, $-(\mathrm{C\underline{H}_2})_9-$), 1·94 (s, 3 H, $-\mathrm{C\underline{H}_3}$), 2·58 (s, 3 H, Ph–$\mathrm{C\underline{H}_3}$), 3·97 (t, 2 H, $-\mathrm{C\underline{H}_2}$–OPh), 4·12 (t, 2 H, –COO–$\mathrm{CH_2}$–), 5·52 and 6·07 (2s, 2 H, $\mathrm{C\underline{H}_2}$=), 6·87–8·11 (m, 7 H, aromatic protons).
4M	78	1·23–1·73 (m, 18 H, $-(\mathrm{C\underline{H}_2})_9-$), 1·95 (s, 3 H, $-\mathrm{C\underline{H}_3}$), 2·42 (s, 3 H, Ph–$\mathrm{C\underline{H}_3}$), 3·96 (t, 2 H, $-\mathrm{C\underline{H}_2}$–OPh), 4·12 (t, 2 H, –COO–$\mathrm{C\underline{H}_2}$–), 5·33 and 6·08 (2s, 2 H, $\mathrm{CH_2}$=), 6·64–8·14 (m, 7 H, aromatic protons).
5M	85	1·30–1·80 (m, 18 H, $-(\mathrm{C\underline{H}_2})_9-$), 1·95 (s, 3 H, $-\mathrm{C\underline{H}_3}$), 2·48 (s, 3 H, Ph–$\mathrm{C\underline{H}_3}$), 3·96 (t, 2 H, $-\mathrm{C\underline{H}_2}$–OPh), 4·14 (t, 2 H, –COO–$\mathrm{C\underline{H}_2}$–), 5·54 and 6·09 (2s, 2 H, $\mathrm{C\underline{H}_2}$=), 6·71–7·63 (m, 7 H, aromatic protons).
6M	81	1·25–1·80 (m, 18 H, $-(\mathrm{C\underline{H}_2})_9-$), 1·94 (s, 3 H, $-\mathrm{C\underline{H}_3}$), 2·49 (s, 3 H, Ph–$\mathrm{C\underline{H}_3}$), 3·96 (t, 2 H, $-\mathrm{C\underline{H}_2}$–OPh), 4·14 (t, 2 H, –COO–$\mathrm{CH_2}$–), 5·54 and 6·09 (2s, 2 H, $\mathrm{C\underline{H}_2}$=), 6·70–7·59 (m, 7 H, aromatic protons).

solution of a monomer (10 per cent wt/vol) and an initiator (AIBN, 1 mol % versus monomer), was degassed under vacuum and finally filled with nitrogen. All polymerizations were carried out at 65°C for 24 h. After the reaction time, the obtained polymers were precipitated in methanol, filtered, purified by several reprecipitations from tetrahydrofuran solutions into methanol. The characterization of the resulting polymers **1P–6P** is presented in table 2.

The authors are grateful to the National Science Council of the Republic of China (NSC-83-0511-E007-01) for its financial support of this work.

References

[1] McArdle, C. B., 1989, *Side Chain Liquid Crystal Polymers* (Blackie).

[2] Meredith, G. R., VanDusen, J. G., and Williams, D. J., 1982, *Macromolecules*, **15**, 1385.

[3] Ye, C., Minami, N., Marks, T. J., Yang, J., and Wong, G. K., 1988, *Macromolecules*, **21**, 2899.

[4] DeMartino, R. N., Choe, E. W., Khanarian, G., Hass, D., Leslie, T., Nelson, G., Stamatoff, J., Steutz, D., Teng, C. C., and Yoon, H., 1988, *Nonlinear Optical and Electroactive Polymers*, edited by P. N. Prasad and D. R. Ulrich (Plenum)), p. 169.

[5] Yitzchaik, S., Berkovic, G., and Krongauz, V., 1990, *Macromolecules*, **23**, 3539.

[6] Chen, M., Yu, L., and Dalton, L. R., 1991, *Macromolecules*, **24**, 5421.

[7] Prasad, P. N., and Williams, D. J., 1991, *Introduction to Nonlinear Optical Effects in Molecules and Polymers* (Wiley).

[8] Hsieh, C. J., Wu, S. H., Hsiue, G. H., and Hsu, C. S., 1994, *J. polym. Sci. polym. Chem.*, **32**, 1077.

[9] Ungnade, H. E., and Orwoll, E. F., 1955, *Org. Synth. Coll.*, **3**, 130.

[10] Niemann, C., Mead, J. F., and Benson, A. B., 1941, *J. Am. Chem. Soc.*, **63**, 609.

[11] Ames, D. E., Bull, D., and Takundwa, C., 1981, *Synthesis*, p. 364.

[12] Percec, V., and Pugh, C., 1989, *Side Chain Liquid Crystal Polymers*, edited by C. B. McArdle (Blackie), Chap. 3, p. 30.

[13] Stevens, H., Rehage, G., and Finkelmann, H., 1984, *Macromolecules*, **17**, 851.

[14] Davidson, P., and Levelut, A. M., 1992, *Liq. Crystals*, **11**, 469.

[15] Noel, C., 1989, *Side Chain Liquid Crystal Polymers*, edited by C. B. McArdle (Blackie), Chap. 6, p. 185.

[16] Sutherland, H. H., Alladib, Z., Gray, G. W., Lacey, D., Nestor, G., and Toyne, K. J., 1988, *Liq. Crystals*, **3**, 1293.

[17] Hsieh, C. J., and Hsiue, G. H., 1994, *Liq. Crystals*, **16**, 469.